Mechanical and biochemical properties of human cervical tissue

K.M. Myers [a]
A.P. Paskaleva [a]
M. House [b]
S. Socrate [a] *

[a] Department of Mechanical Engineering, Massachusetts Institute of Technology, Cambridge, MA 02139, USA
[b] Division of Maternal Fetal Medicine, Tufts-New England Medical Center, Boston, MA 02108, USA

* Corresponding author. Tel.: +1 617 452 2689; fax: +1 617 258 8742.

Abstract

The mechanical integrity of cervical tissue is crucial for maintaining a healthy gestation. Altered tissue biochemistry can cause drastic changes in the mechanical properties of the cervix and contribute to premature cervical dilation and delivery. We present an investigation of the mechanical and biochemical properties of cervical samples from human hysterectomy specimens. Three clinical cases were investigated: nonpregnant hysterectomy patients with previous vaginal deliveries; nonpregnant hysterectomy patients with no previous vaginal deliveries; and pregnant hysterectomy patients at time of cesarean section. Tissue samples were tested in confined compression, unconfined compression and tension. Cervical tissue samples for the three clinical cases were also subjected to biochemical analysis. Biochemical assays measured cervical tissue hydration, collagen content, collagen extractability and sulfated glycosaminoglycan (GAG) content. Results from the mechanical tests indicate that cervical stroma has a nonlinear, time-dependent stress response with varying degrees of conditioning and hysteresis depending on its obstetric background. It was found that the nonpregnant tissue was significantly stiffer than the pregnant tissue in both tension and compression. Further, collagen extractability, sulfated GAG content and hydration were substantially higher in the pregnant tissue. This study is the first important step towards the attainment of an improved understanding of the complex interplay between the molecular structure of cervical tissue and its macroscopic mechanical properties.

Keywords

Cervix; Cervical maturation; Preterm delivery; Cervical biochemistry; Cervical insufficiency

1. Introduction

The human uterine cervix is a passive organ located at the lower end of the uterus (Fig. 1) whose mechanical response during gestation has a critical influence on the outcome of the pregnancy. It has a dual structural function: prior to term, the cervix must stay closed to allow the fetus normal

development (Fig. 1A); and at term, the cervix must dilate under the influence of uterine contractions to allow the fetus passage (Fig. 1B). This dual mechanical functionality is reflected in the changing mechanical properties of the cervical stroma. Firm and rigid at the beginning of pregnancy, the cervix undergoes progressive remodeling during gestation until it is noticeably soft at term. This drastic change in tissue properties is the physical manifestation of a complex biochemical process commonly referred to as cervical maturation (or ripening). The clinical implications of an impaired cervical function are well known to clinicians. For example, cervical insufficiency is a condition in which the cervix softens and dilates prematurely in the absence of apparent uterine contractions. Cervical insufficiency can lead to preterm delivery and in many cases causes extremely premature birth [1]. At the other end of the biomechanical spectrum, a cervix that fails to dilate at term can result in substantial maternal and fetal morbidity [2].

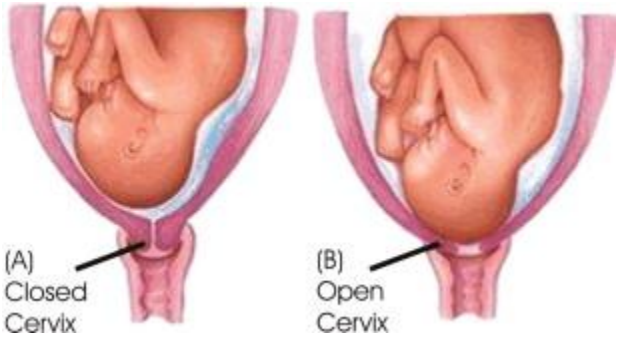

Fig. 1. The cervix uteri during pregnancy (A) and at delivery (B).

Biochemical mechanisms of cervical softening have interested investigators in the obstetric community for many years [3] and [4]. The extracellular matrix (ECM) of the cervical stroma is the load-bearing component of the cervical tissue [5]. Smooth muscle constitutes less than 15% of the stroma [6] and does not appear to contribute to cervical strength [7]. The ECM of the stroma is similar to other fibrous connective tissues. The primary constituents are type I and type III collagen [8], hyaluronan (HA) and proteoglycans (PGs) [9], elastin [10] and water.

Several lines of evidence implicate disruption of the collagen network as the microstructural mechanism associated with macroscopic cervical softening. Light and electron microscopy studies [11], [12] and [13] and collagen solubility experiments [8], [9], [14] and [15] show that softening of the cervix is associated with collagen fiber disruption and a decrease in collagen crosslinking. HA, matricellular proteins and PGs are also suspected to play an important role in cervical maturation [16] by influencing the collagen and tissue architecture. The observed increase in HA content during pregnancy, in particular nearing delivery, has been directly related to an increase in cervical hydration and disorganization of the collagen network [17]. A number of studies on animal models have used targeted gene disruption to identify ECM components with a prominent effect on collagen morphology and tissue properties. In particular, studies on decorin [18] and thrombospondin 2 [19] substantiate the hypothesis of a direct involvement of these ECM components in the regulation of cervical tissue properties. Recent studies indicate that the biochemical cascade leading to cervical maturation can be activated by mechanical deformation of the cervical fibroblast cells [20] and [21].

Few studies have been able to correlate biochemical variables to stroma mechanical properties. Rather, investigators have demonstrated correlations between stroma biochemistry and clinical variables. Studies have shown a correlation between tissue hydration, collagen extractability and obstetric history. Pregnant cervical tissue is more hydrated and has higher collagen extractability than nonpregnant tissue [14], [15] and [23]. Furthermore, obstetricians know that prior vaginal birth increases the speed of a subsequent birth, presumably via an effect on the cervical stroma [22]. Hence, it is not surprising that increasing parity (number of previous vaginal deliveries) has been shown to correlate with a weaker collagen network [23] and [15]. Cervical insufficiency was found to be associated with increased collagen extractability [15]. In contrast, protracted labor has been associated with higher collagen content and lower extractability [24]. Collagen crosslinking has been investigated in vivo with a noninvasive autofluorescence tool [25]. The cervical autofluorescence signature changes with increasing gestational age, presumably because fewer collagen crosslinks are present.

The number of investigations on quantitative measurements of the tissue mechanical properties ("softness") is very limited, especially when compared to the substantial number of studies dedicated to cervical tissue biochemistry. Most studies employed animal models (e.g. [19], [26] and [27]), while a small number of investigations performed on human tissue in tension did confirm that the pregnant cervix is significantly more deformable compared to the nonpregnant cervix [14] and [28].

In current clinical practice, the biomechanical status of the cervix is assessed in terms of a subjective scoring system introduced by Bishop [29]. Objective methods for measuring cervical softness during pregnancy have not found their way into clinical practice, although tonometric techniques have been proposed [30] and [31]. These tonometric measurements demonstrated that cervical softening occurs in a gradual fashion throughout gestation. More recently, an aspiration device was developed to measure cervical softness [32]. This study on nonpregnant human cervical tissue concluded that variations in the mechanical properties of the cervix measured in vivo and in vitro were negligible.

The long-term objective of our study is to investigate cervical mechanical function during pregnancy. A crucial component of this study is an investigation of the structure–property relations for the constitutive behavior of cervical tissue, connecting changes in biochemical composition of the tissue to the observed variations in its mechanical properties. The role of different tissue components can be more prevalent in specific modes of deformation (e.g. collagen in tension, glycosaminoglycans (GAGs) in compression). In order to elucidate these effects, we needed to develop a stringent experimental protocol to collect comprehensive data on the biochemical composition and mechanical properties of ex vivo tissue samples under different loading modes (e.g. tension, confined compression, unconfined compression) and loading histories (e.g. constant strain rate, ramp-relaxation).

Notwithstanding the abundant number of studies on cervical tissue biochemistry, the disparity of methods and protocols yields large discrepancies in the results reported in the literature. In this study, we aimed at identifying appropriate biochemical assays to determine collagen content and collagen extractability in human cervical specimens. Total sulfated GAG concentrations were

also determined, while protocols to determine the specific concentrations of individual GAG types are the subject of current investigation.

Here we present preliminary results of our experimental studies and discuss relevant issues pertaining to the established protocols. We obtained tissue samples from hysterectomy specimens from both cesarean deliveries and from premenopausal surgery. Although this preliminary study involved a limited number of specimens, the results of our investigation qualitatively confirm the expected trends concerning the influence of gestational age and obstetric history on mechanical and biochemical measurements. Further, the results presented here provide the first quantitative mechanical measurements of cervical stroma in confined and unconfined compression. These results are the foundation for the development of an appropriate constitutive model for cervical stroma and will guide future studies to further explore the tissue's anisotropic response in compression and tension.

2. Methods

2.1. Tissue harvesting and specimen preparation

Hysterectomy specimens from pre-menopausal women with benign gynecological conditions were obtained from the Tufts–New England Medical Center. Two cervices were obtained from cesarean hysterectomy patients. Both patients underwent cesarean hysterectomy because of suspected placenta accreta and did not labor. Nonpregnant cervices were categorized according to parity and labeled NPND for women with no previous vaginal deliveries and NPPD for women with previous vaginal deliveries. The pregnant specimens were labeled PCS. Please refer to Table 1 for abbreviation definitions and to Table 2 for specific patient obstetric history. Approval from the Institutional Review Board was obtained from both the Tufts–New England Medical Center and the Massachusetts Institute of Technology prior to initiating the study.

Table 1. Sample labels

Obstetric history	**Abbreviation**
Non-pregnant: no previous vaginal deliveries	NPND
Non-pregnant: previous vaginal deliveries	NPPD
Pregnant: taken at time of cesarean section	PCS

Table 2. Patient-specific obstetric history

Patient	**Age**	**G**	**P**	**Hysterectomy indication**	**Obstetric history**	**Labor?**	**Endometrial pathology**
NPND Patient 1	37	0	0	Fibroid uterus		No	Proliferative
NPND Patient 2	38	4	4	DUB	C/Sx4	No	Secretory
NPND Patient 3	43	4	3	Fibroid uterus	C/Sx3	Dilated to 4 cm in first pregnancy. Did not labor in second and	Secretory

						third pregnancies	
NPND Patient 4	37	0	0	Fibroid uterus		No	Proliferative
NPND Patient 5	35	0	0	Fibroid uterus		No	Secretory
NPPD Patient 1	53	2	2	Fibroid uterus	NSVDx2	Yes	Proliferative
NPPD Patient 2	43	2	2	DUB	NSVDx2	Yes	Dysynchronous
NPPD Patient 3	46	1	1	Fibroid uterus	NSVDx1	Yes	Proliferative
PCS Patient 1	33	4	2	34 weeks gestation; suspected placenta increta	C/Sx2	No, C/S performed prior to labor	Increta confirmed
PCS Patient 2	32	5	5	37 weeks gestation; suspected placenta accreta	C/Sx5	No, C/S performed prior to labor	Accreta confirmed

G = gravida, P = para, DUB = dysfunctional uterine bleeding, NSVD = normal spontaneous vaginal delivery, C/S = cesarean section.

The uterus and cervix were excised from the patients and placed on ice. A custom-designed stainless steel sectioning tool (Fig. 2A) was used to obtain from each cervix four 4 mm parallel disks perpendicular to the inner canal. Each cervical slice was labeled to distinguish its position relative to the internal and external os (Fig. 2B). Note that the 2 cm of cervix closest to the external os was not tested because this portion was reserved for pathological examination. The cervical tissue slices were stored flat at −80 °C. Preliminary tests performed on fresh and previously frozen tissue from the same cervical slice [37] confirmed that freezing does not alter the mechanical properties, a result consistent with similar findings for cartilage (e.g. [33]). Prior to testing, each 4 mm slice was thawed for approximately 3 min in phosphate-buffered saline (PBS) at an ionic concentration of 0.15 M.

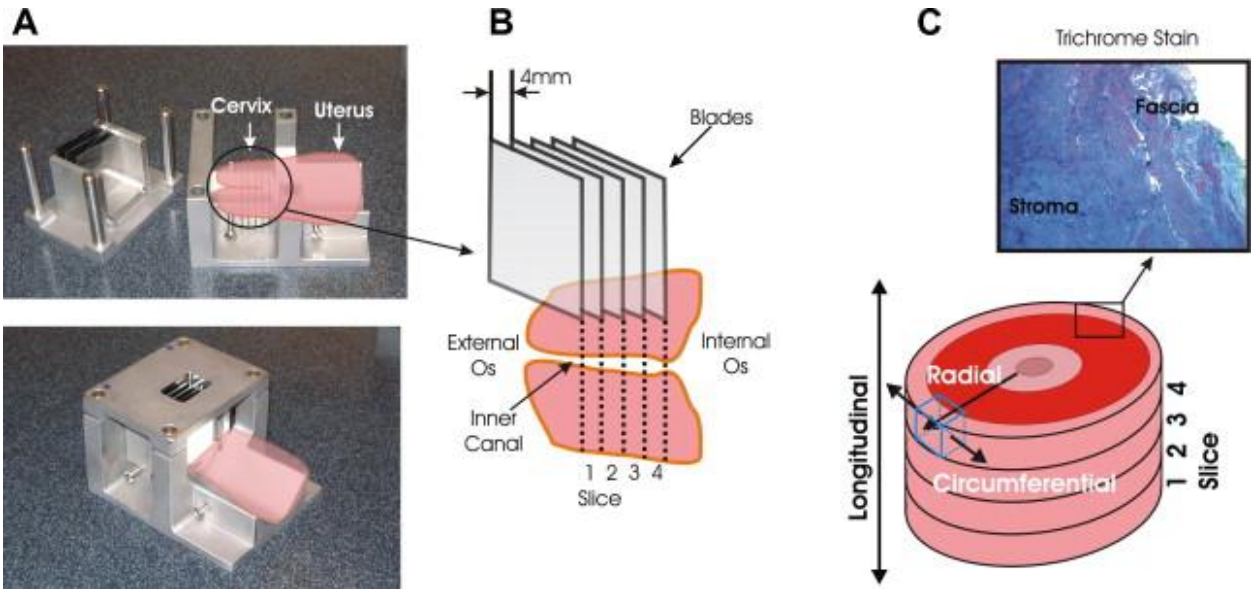

Fig. 2. Specimen preparation. (A) Stainless steel sectioning tool. (B) Cervical slice labeling convention and blade orientation. (C) Cervical tissue. The mucosa is the soft cellular layer lining the cervical canal, and the fascia is the soft cellular layer surrounding the stroma. The stroma is the firm fibrous inner core. Conventions for anatomical orientation within the cervix are indicated.

Mechanical and biochemical specimens were cut exclusively from the cervical stroma. The location of the cervical stroma in relation to the cervical mucosa and fascia is illustrated in Fig. 2C. For compressive mechanical tests, cylindrical specimens were cut with an 8 mm biopsy punch at the same radial location for each slice, with the cylinder axis parallel to the inner canal. Care was taken in labeling the samples according to their anatomical site, as data in the literature [28] indicate some variation in mechanical properties with longitudinal position along the axis of the cervix, and radial distance from the cervical canal. For tension mechanical experiments, two concentric circular blades were used to obtain from each slice a singular ring of stroma of ~6–8 mm inner diameter and ~16–18 mm outer diameter. For biochemical specimens, ~20 mg of tissue adjacent to the location of the mechanical specimens were excised from the stroma.

Each cervical slice yielded compression specimens (1–3 specimens, depending on the visual homogeneity of individual slices) or a single tension specimen, as well as several biochemical specimens. The mechanical specimens were weighed and equilibrated overnight in PBS at 4 °C, and the biochemical specimens were stored at −80 °C until time of pulverization.

2.2. Mechanical testing

All tests were conducted on a universal material testing machine (Zwick Z2.5/TS1S, Ulm, Germany) with the specimens immersed in a PBS bath in custom-designed acrylic fixtures (Fig. 3B). A 20 N load cell was used to collect compression data, and a 500 N load cell was used to collect tension data. Video extensometer data were collected with a Qimaging Retiga 1300 CCD camera equipped with a 200 mm f/4 Nikkor lens. Strain data were obtained with digital image correlation (DIC) techniques using Correlated Solutions VIC-2D (v. 4.4.0) software.

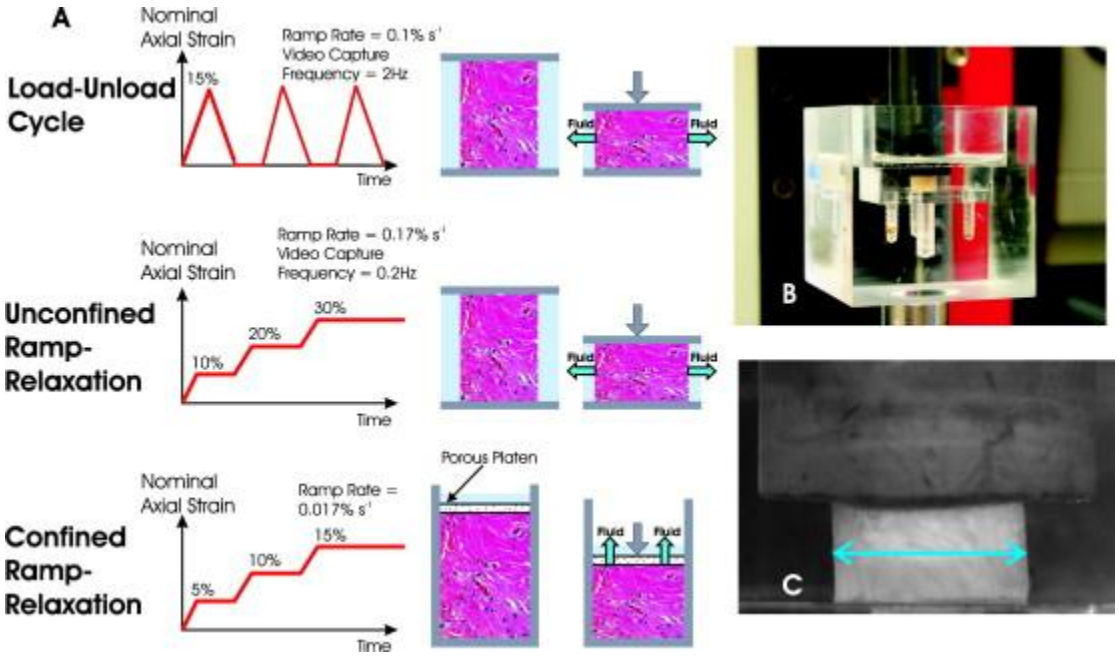

Fig. 3. Compression test protocol. (A) Imposed deformation history for each testing mode. (B) Cervical specimen in compression fixture. (C) Cervical specimen in unconfined compression. Radial stretch history is recorded by a video extensometer.

Measurement variability is inherent in the Zwick load cell and video extensometer analysis. The resolution of the 20 N Zwick load cell is ±0.001 N (~0.01 kPa for an 8 mm diameter specimen), and the resolution of the 500 N Zwick load cell is ±0.025 N (~1.0 kPa for a typical ring geometry). The tolerance of the lateral stretch measurements is a function of the resolution and contrast quality of the video extensometer image. A full discussion of error calculations for the video extensometer can be found in Parson [34]. For our unconfined compression tests an estimate of error was obtained by performing a lateral stretch analysis multiple times for the same image data. The variation in strain due to noise in the video extensometer analysis was found to be within ±1% for testing conditions typical of the unconfined compression configuration. For the ring tension tests, a preliminary image-analysis experiment was conducted using rigid body motion to calibrate the strain error for a particular speckle pattern and camera resolution. For the resolution and speckle pattern used in the tension experiments, the strain error was found to be within ±0.1%.

All mechanical specimens were equilibrated overnight in PBS at 4 °C, weighed and measured prior to testing. A discussion of the motivation and implications for this equilibration procedure, which alters the hydration level of the tissue, is presented in Section 4.1.

Each compression specimen was subjected to three different testing modes: load–unload cycle; unconfined ramp-relaxation; and confined ramp-relaxation. A preload of 0.005 N (corresponding to a compressive stress of 100 Pa) was imposed on each sample prior to testing in order to accurately determine the sample thickness and, for the confined compression tests, improve confinement. Fig. 3A illustrates the imposed deformation histories for the three tests. The

compression testing protocol for each specimen consisted of the following sequence of tests: (1) load–unload cycle, (2) unconfined ramp-relaxation, (3) load–unload cycle, (4) confined ramp-relaxation. Each specimen was first loaded in unconfined compression to 15% axial-engineering strain and unloaded to 0% strain at a constant engineering strain rate of 0.1% s−1. This load–unload cycle was repeated three times. After re-equilibration in an unloaded state for at least 30 min in PBS at 4 °C, the specimen was subsequently subjected to an unconfined ramp-relaxation test to axial-engineering strain levels of 10%, 20% and 30% with a ramp strain rate of 0.17% s−1. Each strain level was held for 30 min to measure the relaxation response of the tissue. After re-equilibration in an unloaded state for at least 30 min in PBS at 4 °C, the load–unload cycle test was repeated. The measured response was compared to the response recorded in the first load–unload test to verify that the specimen had not undergone any damage or degradation that might alter its mechanical response. The specimen was then allowed to re-equilibrate for 30 min in PBS. After equilibration, the specimen was placed in an 8 mm impermeable rigid well and subjected to a confined ramp-relaxation test to axial strain levels of 5%, 10% and 15% with a ramp strain rate of 0.017% s−1. Each strain level was held for 30 min to measure the relaxation response of the tissue. The history of radial stretch for the unconfined compression tests (both load–unload cycles and ramp-relaxation) was recorded using the video extensometer. The video capture frequencies for the load–unload cycle and the ramp-relaxation test were 2 and 0.2 Hz respectively. Fig. 3C shows a typical video image for an unconfined compression test.

For tensile tests, prior to loading, an airbrush pattern was applied to the ring-shaped tension specimens using India ink. A representative speckle pattern density is illustrated in Fig. 4A. The speckled cervical rings were extended along a diameter using 5 mm wide woven Kevlar strips, which were looped around the specimen and gripped in tensile jaws (Fig. 4). This testing configuration was selected to reduce stress concentration in the gripped region of the specimen, while adding negligible axial compliance to the grip assembly. Specimen and grip assembly were immersed in a PBS bath in an acrylic fixture (Fig. 4B). The inner diameter of the cervical ring was elongated at a rate of 0.05 mm s−1. Multiple tension-loading cycles were imposed on each specimen, with 30 min of equilibration time between each cycle. Images of the deforming specimen were recorded at a frequency of 10 Hz. The two-dimensional strain field was obtained for the two central regions of the specimen as indicated in Fig. 3A using the Correlated Solutions Vic 2-D DIC software [34]. Axial and lateral stretch histories were then averaged for these mostly uniform regions of deformation. Based on lateral stretch history and initial specimen dimensions, a (true) axial stress history for the central region of the specimen was estimated.

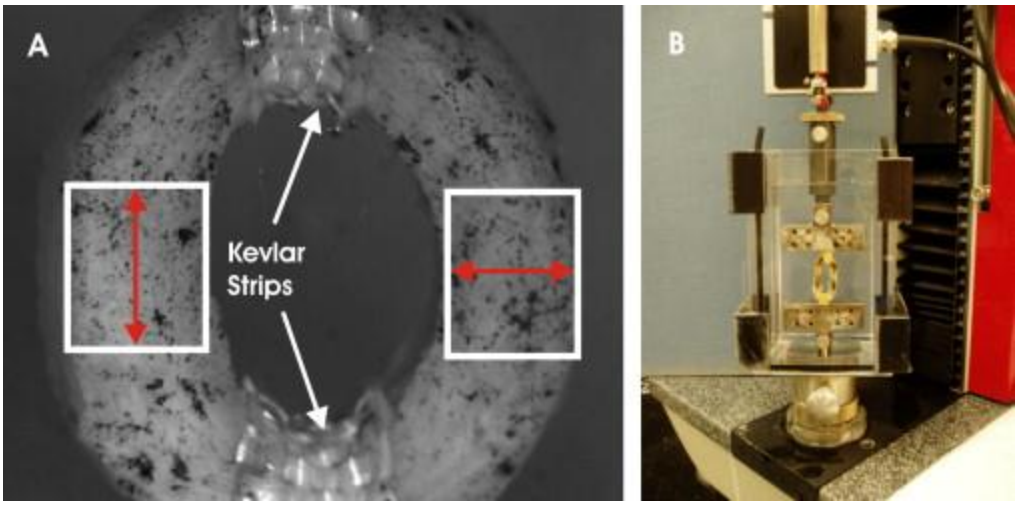

Fig. 4. Tension test configuration. (A) Representative speckle pattern for cervical tension specimens. Axial and lateral stretch histories are recorded for the boxed regions indicated in the figure, where the deformation is sufficiently homogeneous, and the stress state more closely approaches uniaxial tension. (B) Experimental fixture for cervical tension test. Two strips of woven Kevlar are looped around the specimen and gripped in tensile jaws.

2.3. Biochemical analysis

Cervical tissue was defatted and homogenized prior to all biochemical assays. Samples were defatted in acetone for 3 days at 4 °C and then homogenized by pulverizing approximately 20 mg of wet tissue in a stainless steel chamber cooled with liquid nitrogen. Collagen content was measured using a standard hydroxyproline assay [35]. The hydroxyproline content was obtained using a colorimetric procedure, and was converted into collagen content using a mass ratio of collagen to hydroxyproline of 7.64:1. Collagen content was normalized by tissue dry weight.

Collagen extractability was measured by extracting approximately 20 mg of wet pulverized tissue in 0.5 M acetic acid containing 1 mg ml−1 of pepsin (150 μl mg−1 wet tissue) for 3 days at 4 °C. The sample was centrifuged at 15,000g for 1 h and the supernatant and tissue pellet were stored at −80 °C. The hydroxyproline content was measured in the tissue pellet and the supernatant. The extractability is defined as the fraction of hydroxyproline in the supernatant compared to the total amount of hydroxyproline.

Sulfated GAG content was measured using a standard dimethylmethylene blue (DMB) assay [36] with chondroitin-6-sulfate (Sigma–Aldrich) as the standard. Approximately 20 mg of wet cervical tissue was pulverized and then freeze-dried overnight. The dry tissue was then incubated overnight in 1 ml of 0.1 mg ml−1 solution of proteinase K (Roche Applied Science). After incubation, the tissue was assayed for sulfated GAGs using a 1,9-dimethylmethylene blue dye (Polyscience Inc.).

3. Results

Mechanical and biochemical properties were measured for the NPPD, NPND and PCS (Refer to Table 1 for abbreviation definitions) clinical cases and averaged according to this classification. Nc represents the number of cervices and Ns represents the total number of specimens tested for each clinical case.

The appearance and the texture of cervical tissue were visibly different for the three clinical cases. The pregnant tissue was noticeably softer and the collagen network appeared to be loosely connected, in agreement with observations reported in the literature [4]. The nonpregnant tissue appeared fibrous, with a densely connected collagen network, especially for the NPND clinical cases.

3.1. Mechanical testing

Compression tests were performed, on cylindrical specimens, and Fig. 5 shows the averaged stress responses of the tissue to the load–unload compression cycles for the three clinical cases. The averaged peak stresses in Fig. 5 reflect an order of magnitude difference between the averaged responses for the NPND and PCS cases, and a substantial difference between the NPND and NPPD responses. Standard variations in peak stress (at 15% axial strain) for the three obstetric histories are reported in Table 3.

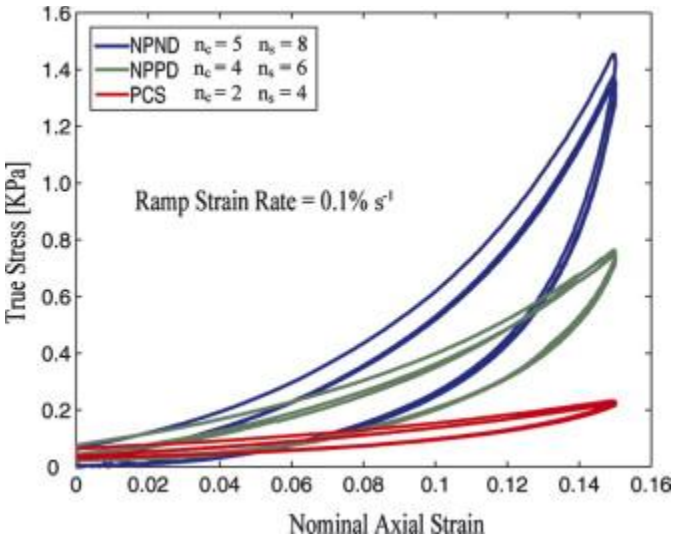

Fig. 5. Cervical stroma response to uniaxial compression cycles. Experimental curves were averaged for each obstetric case.

Table 3. Standard variation in peak stress values (at 15% axial strain) for the load–unload compression tests

Obstetric case	**Nc**	**Ns**	**Standard variation in peak stress (kPa)**
NPND	5	7	±1.2
NPPD	3	9	±0.4
PCS	2	3	±0.1

For constant strain rate load–unload cycles, the material displays a nonlinear response, with marked hysteresis. The first loading cycle is consistently associated with a stiffer response and more substantial hysteresis. The response in subsequent loading ramps becomes more compliant, while the unloading response is not substantially altered between cycles. This softening behavior with subsequent deformation cycles has been observed in other classes of soft tissues and is often referred to as "conditioning".

Fig. 6 shows the averaged stress responses of the tissue to the ramp-relaxation tests in unconfined and confined compression for the three clinical cases. Standard variations in peak stresses and equilibrium stresses are reported in Table 4 and Table 5. There is a trend towards significantly decreased amplitude in the stress response of pregnant tissue when compared to nonpregnant tissue ($p = 0.1$, Student's t-test) and in NPPD tissue when compared to NPND tissue ($p = 0.1$, Student's t-test). These findings are consistent with the clinical observation that pregnant tissue is softer than nonpregnant tissue, and women with previous deliveries tend to have a softer cervix when compared to women who have not delivered vaginally.

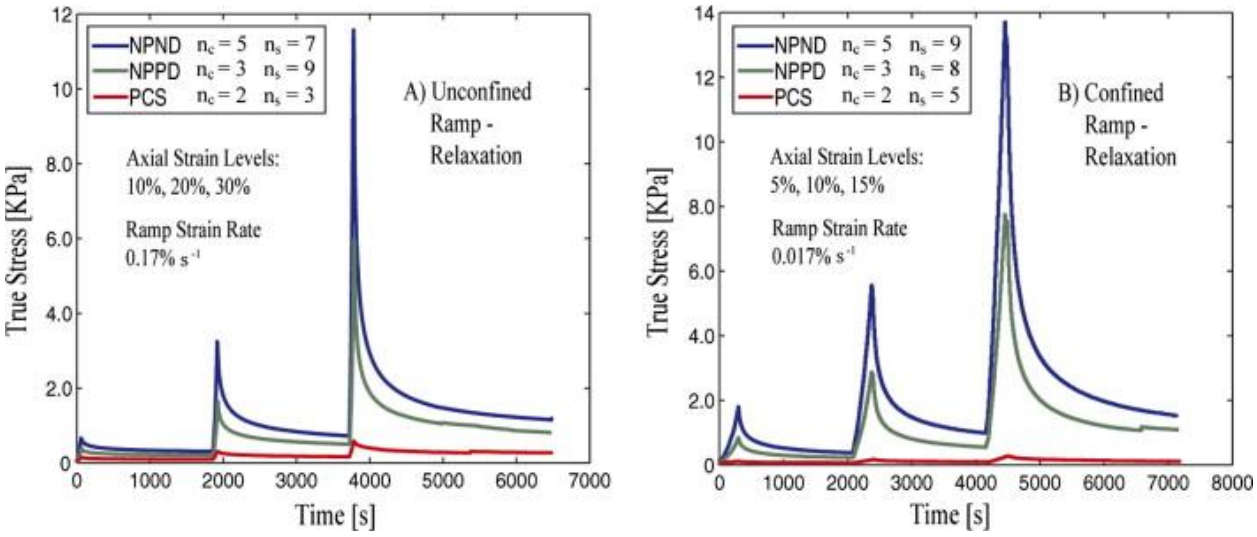

Fig. 6. Cervical stroma response to ramp-relaxation in (A) unconfined compression, and (B) confined compression. Experimental curves were averaged for each obstetric case.

Table 4. Peak and equilibrium stresses for unconfined compression

Obstetric case	**Nc**	**Ns**	**10% Peak (kPa)**	**20% Peak (kPa)**	**30% Peak (kPa)**	**10% Equilibrium (kPa)**	**20% Equilibrium (kPa)**	**30% Equilibrium (kPa)**
NPND	5	7	0.66 ± 0.46	3.2 ± 3.2	12 ± 14	0.31 ± 0.24	0.72 ± 0.53	1.2 ± 0.78
NPPD	3	9	0.39 ± 0.38	1.6 ± 2.3	6.0 ± 9.6	0.21 ± 0.17	0.50 ± 0.39	0.82 ± 0.76
PCS	2	3	0.15 ± 0.12	0.30 ± 0.24	0.56 ± 0.64	0.10 ± 0.06	0.17 ± 0.15	0.28 ± 0.23

Table 5. Peak and equilibrium stresses for confined compression

Obstetric case	Nc	Ns	5% Peak (kPa)	10% Peak (kPa)	15% Peak (kPa)	5% Equilibrium (kPa)	10% Equilibrium (kPa)	15% Equilibrium (kPa)
NPND	5	9	1.8 ± 3.7	5.6 ± 9.4	14 ± 17	0.38 ± 0.57	0.99 ± 1.1	1.5 ± 1.4
NPPD	3	8	0.82 ± 2.0	2.9 ± 5.7	7.8 ± 13	0.23 ± 0.40	0.55 ± 0.78	1.1 ± 1.2
PCS	2	5	0.12 ± 0.07	0.17 ± 0.10	0.28 ± 0.18	0.07 ± 0.07	0.10 ± 0.08	0.12 ± 0.08

Averaged transverse stretch histories for the three clinical cases in unconfined ramp-relaxation tests are reported in Fig. 7. The results indicate that the specimens undergo a substantial volume change in unconfined compression tests. Error bars are not indicated in the figure to avoid cluttering, but typical variations among specimens were of order ±0.03. This large variation in transverse stretch measurements was probably due to tissue anisotropy and specimen orientation inconsistencies: the loading direction is "anatomically" consistent for all specimens (longitudinal in the cervix, i.e. parallel to the direction of the inner canal, see Fig. 2). However the orientation of each specimen with respect to radial and circumferential direction in the cervix was not recorded or marked on each specimen, and the transverse direction for which the stretch was recorded was not anatomically consistent among specimens.

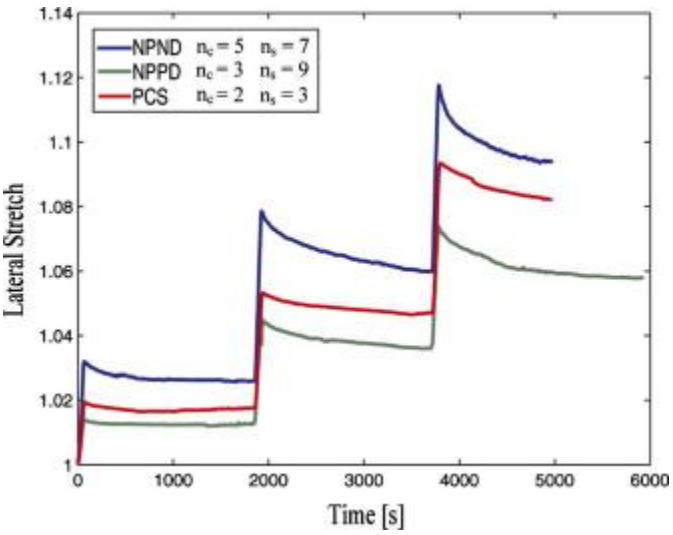

Fig. 7. Radial transverse stretch of specimens subjected to ramp-relaxation unconfined compression. Experimental curves were averaged for each obstetric case.

Fig. 8 and Fig. 9 show the results for preliminary tension experiments conducted on cervical specimens with different obstetric backgrounds and different anatomical locations. Fig. 8. shows results from three specimens taken from cervices with different obstetric backgrounds. Fig. 9 shows results from two specimens taken from the same pregnant cervix, where the specimens were taken from different anatomical sites. Results are presented in terms of averaged true stress vs. averaged axial stretch in the central regions of the specimens, as discussed in Section 2. Fig. 8 shows that pregnant tissue is found to be orders of magnitude more compliant than nonpregnant tissue. This result confirms trends identified in the compression tests. Further, Fig. 8 indicates no significant difference in the stress–stretch response for the two nonpregnant cases.

Fig. 9 shows that the stress response of cervical tissue is dependent on anatomical site. The specimen taken closer to the external os has a stiffer stress response when compared to the specimen taken closer to the internal os. This result is consistent with clinically observed progression in cervical ripening.

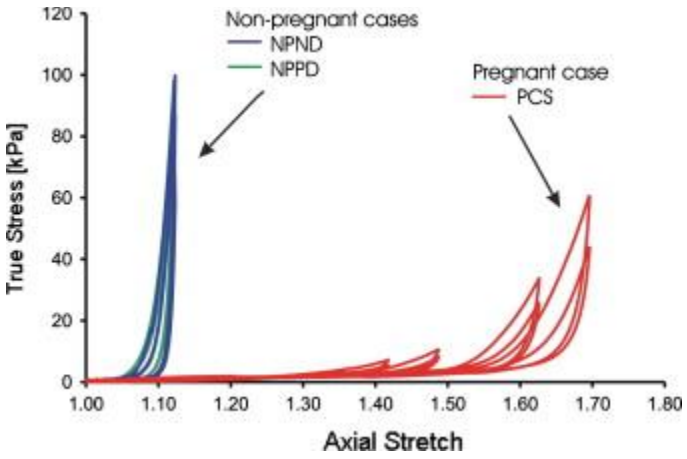

Fig. 8. Cervical stroma response in tension for three specimens from three patients with different obstetric backgrounds. Between each cycle, the unloaded specimen was equilibrated for 30 min in PBS.

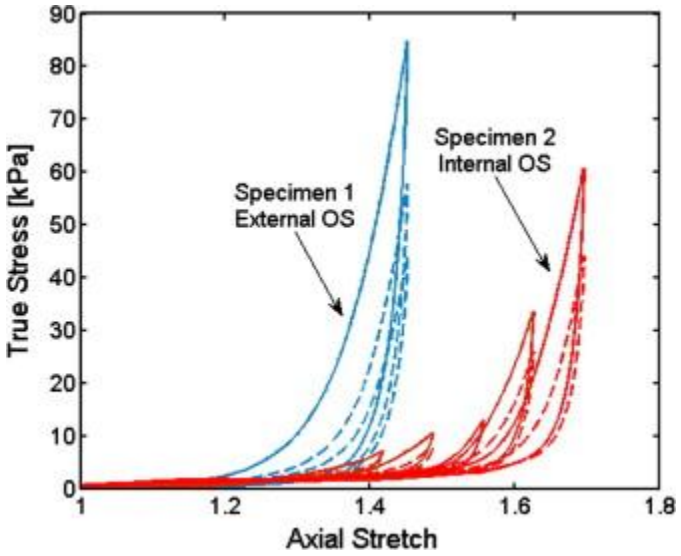

Fig. 9. Cervical stroma response in tension for two specimens from a single pregnant cervix. Specimen 1 was taken close to the external OS, and specimen 2 was taken close to the internal OS. Between each cycle, the unloaded specimen was equilibrated for 30 min in PBS.

The tensile response of the tissue is extremely nonlinear, with a degree of hysteresis that increases with the level of applied deformation. Similar to the findings for compressive axial deformation, the response of nonpregnant cervical tissue experienced a degree of conditioning during the first loading cycle, and then stabilized in subsequent cycles. Conversely, the pregnant tissue continued to elongate with each loading cycle.

3.2. Biochemical analysis

Cervical tissue samples for the three (NPND, NPPD and PCS) clinical cases were subjected to biochemical analysis. Biochemical assays measured cervical tissue hydration, collagen content, collagen extractability and sulfated GAG content. Table 6 reports the biochemical content measured for the three clinical cases. Data were averaged among cervices with the same obstetric history. Table 6 gives both average values and standard deviations over the number of samples (Ns) analyzed for each assay. A significant ($p < 0.05$, Student's t-test) difference in hydration and collagen extractability was established between pregnant and nonpregnant specimens. Pregnant tissue was more hydrated and its collagen network was more soluble in acetic acid when compared to the nonpregnant tissue samples. There was no statistically significant difference in hydration and collagen extractability when comparing the two nonpregnant cases. Further there was no significant difference in collagen content among all clinical cases. Lastly, a limited number of pregnant samples were tested for sulfated GAG content. The results indicate a substantial increase in sulfated GAG content in pregnant tissue when compared to nonpregnant tissue. There was no difference measured in sulfated GAGs when comparing the two nonpregnant cases.

Table 6. Results of biochemical assays

Obstetric case	**Hydration**	**Collagen content (% per dry weight)**	**Collagen extractability**	**Sulfated GAGs (% per dry weight)**
NPND	73.8 ± 5.9%	71.0 ± 8.6%	28.6 ± 5.9%	1.20 ± 0.74%
	Nc = 5; Ns = 40	Nc = 3; Ns = 25	Nc = 2; Ns = 6	Nc = 5; Ns = 21
NPPD	76.7 ± 2.0%	77.5 ± 8.3%	33.1 ± 6.1%	1.53 ± 0.16%
	Nc = 8; Ns = 80	Nc = 5; Ns = 18	Nc = 4; Ns = 8	Nc = 4; Ns = 20
PCS	87.2 ± 1.6%	77.6 ± 9.8%	78.5 ± 1.1%	5.52 ± 2.29%
	Nc = 1; Ns = 3	Nc = 2; Ns = 8	Nc = 2; Ns = 6	Nc = 1; Ns = 2

4. Discussion

This study had two complementary objectives: (i) the establishment of a stringent experimental protocol to collect data on the biochemical composition and mechanical properties of cervical tissue under different loading modes; (ii) a preliminary investigation of normal ranges of variation in tissue properties for nonpregnant and pregnant patients. Here we discuss the motivation and implications of our testing protocols, discuss the experimental results, explain the sources of variability in the experimental findings, and suggest changes to the current experimental protocol for future studies.

4.1. Discussion of the testing protocol

The motivation behind the selected modes of deformation, strain levels and strain rates arises from physiological considerations, ranges of operation of the test equipment and mechanical modeling concerns. This extensive experimental characterization of the mechanical tissue response was necessary to guide the development of an appropriate constitutive model for cervical stroma [37]. The experimental protocol was designed so as to provide sufficient data to uniquely determine the constitutive material parameters that describe the mechanical behavior of each cervical specimen [37]. The advantage of testing each cervical specimen in both confined

and unconfined compression is that these combined protocols provide sufficient data to characterize the three-dimensional, poroelastic and viscoelastic nature of the tissue response [38], [39] and [40]. Confined compression tests impose larger volume changes, and the experimental response is typically interpreted in a poroelastic framework to provide estimates for the (strain-dependent) hydraulic permeability of the tissue [41]. Unconfined compression tests typically result in larger levels of shear deformation. The three-dimensional behavior of the tissue is captured by the lateral stretch measurements taken by the video extensometer.

The rationale for testing samples along the longitudinal direction in compression tests, and testing samples along the circumferential direction in tensile tests arises, from physiological considerations [42] and [28] and from preliminary results of finite element analyses (FEA) of the loading conditions in pregnant patients [43]. Gravity, intrauterine pressure and the weight of the fetus impose a complex three-dimensional stress state on the cervix: the weight of the fetus gives rise to compression loads in the longitudinal direction, and the resistance to cervical dilation gives rise to tensile loads in the circumferential direction [42] and [43].

Strain levels and strain rates were selected on the basis of preliminary experimental investigations [37]. Strain levels were selected to meet the criteria that they should not cause damage to the specimens, but should be high enough to capture the nonlinearity of the tissue response. Physiologically, the strain rates experienced in vivo by the tissue under time-varying loading conditions (gravity, uterine contractions, etc.) will vary widely among patients. Strain rates for the load–unload cycles and for the ramp loading in relaxation tests reflect the short loading times characteristic of physiological conditions such as uterine contractions and temporary increases in intra-abdominal pressure (e.g. from coughing). The relaxation transient is meant to capture longer-term (and equilibrium) tissue response. The strain rate for the tension test protocol is similar to the rate adopted in the tension tests by Conrad et al. [28]. Also, strain rates were selected so as to meet the following criteria: (i) the load did not exceed the limit of the load cell; (ii) the tissue samples were not damaged during loading; (iii) inertial effects could be neglected; and (iv) the time-dependent nature of the tissue response (hysteresis, relaxation) could be captured. The characteristic relaxation times in confined compression experiments are dominated by the effects of fluid diffusion and are higher than the characteristic relaxation times in unconfined compression. To avoid overloading the specimen and load cell, lower strain levels and strain rates were selected for confined compression tests.

We found that, to obtain repeatable results, a number of precautions were necessary. First, to prevent tissue degradation, the cervical slices were stored at −80 °C at time of excision until the experiments were performed. Second, to eliminate transient effects associated with swelling, mechanical specimens were equilibrated overnight in PBS at 4 °C prior to testing.

The hydration levels of the stroma significantly affect its mechanical response. As mechanical specimens are excised from the surrounding tissue, constraints from the interconnected collagen network are relaxed. Freezing the tissue can also result in partial loss of hydration. When the excised tissue is placed in saline at physiological concentration, the specimen swells to reach a new equilibrium state at a higher hydration level. Typical swelling curves for compression specimens are shown in Fig. 10 where the wet weights of two specimens are plotted as a function of the hydration time in PBS. These curves display a rapid rise in hydration level, immediately

following the placement of the specimen in saline, with exponentially decreasing hydration rates over time. Typical characteristic time constants for this hydration transient (~5 h) are comparable with testing time intervals. If a specimen is not allowed to equilibrate properly prior to testing, the testing results will be confounded by the superposition of effects due to the hydration process.

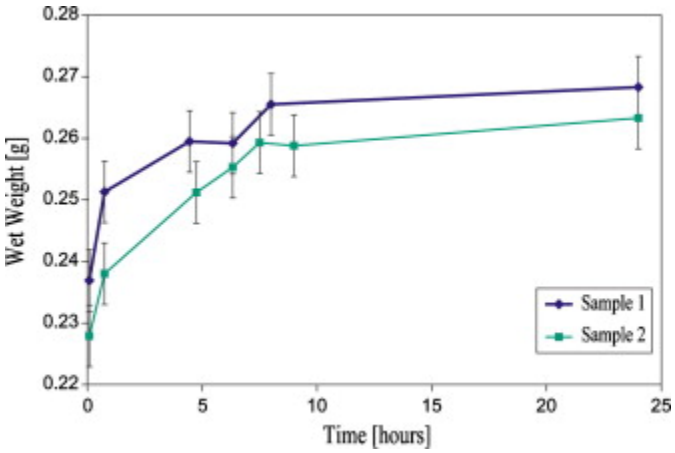

Fig. 10. Swelling curve from two compression specimens obtained from the same cervical slice.

Fig. 11 demonstrates the significant influence of hydration levels on the measured mechanical properties. Two compression samples were excised from the same cervical slice and tested after short hydration intervals (1.5 and 3 h). The sample that was allowed to hydrate for a longer interval displayed a stiffer response. The same specimens were then placed in saline, equilibrated overnight and retested. A noticeably stiffer response was obtained for the fully equilibrated specimens. Interestingly, the sample that had originally appeared stiffer proved to be the more compliant of the two when equilibrated. It could be argued that the adopted equilibration protocol alters the tissue properties from their in vivo state. However, the purpose of this investigation was not to obtain absolute values of tissue properties, but rather to identify overall qualitative features of the tissue response and to investigate relative variations in properties between specimens from patients with different obstetric histories. The equilibration protocol is evenly applied to all samples, and the increased hydration level only affects the amplitude of the stress response and not the qualitative feature of the curves. For the purpose of this investigation, the effects of the equilibration step are therefore inconsequential. In future studies, we propose to use a stronger ionic bath, both in the equilibration and in the mechanical testing procedures, to limit the swelling of the tissue and reach equilibrium hydration levels comparable to the in vivo levels.

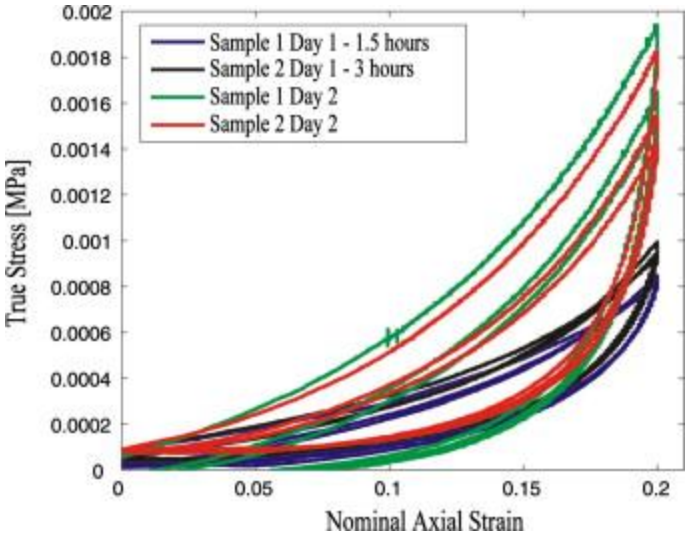

Fig. 11. Uniaxial load–unload compression cycle response for different equilibration times. The two specimens were obtained from the same cervical slice.

4.2. Discussion of results

Many observations about the characteristics of the material response can be used to guide the development of an appropriate constitutive model for the mechanical behavior of cervical stroma. The stress–strain behavior is noticeably nonlinear both in tension and compression, with a much stiffer response when the tissue is loaded in tension: in nonpregnant tissue, for strain levels of approximately 10%, there are two orders of magnitude between the corresponding stress levels in tension (~100 kPa) and compression (~1 kPa). The nonlinearity of the stress–strain behavior is also reflected in the relationship between peak stresses and strains for the ramp-relaxation results in confined and unconfined compression. Conversely, for both unconfined and confined compression tests, and for all three clinical cases, the increase in equilibrium stresses with axial strain was nearly linear. While the peak stress levels for the nonpregnant specimens were an order of magnitude higher than the equilibrium levels, the peak stress levels for the pregnant specimens were not substantially higher than the equilibrium levels. Since fluid diffusion controls the transient peak response, this result is consistent with qualitative observations of the tissue morphology: much higher hydraulic permeability coefficients are probably associated with the loosely connected pregnant tissue.

The data suggest that the relaxation behavior is associated with at least two separate mechanisms. The first mechanism occurs in a very short time interval (~10 s) with substantial relaxation immediately following the loading ramp. After this sharp stress drop, the stress continues to decrease at a much lower rate, suggesting the presence of a second relaxation mechanism with a much larger characteristic decay time. A relaxed state is only partially attained at the end of the 30 min relaxation interval. Also, relaxation times are slightly reduced for the unconfined compression cases, possibly due to differences associated with the transient diffusion of interstitial fluid. This difference arises because the surface of the unconfined specimens in contact with the bathing solution is nearly doubled. Furthermore, the confined compression configuration imposes a volumetric strain on the tissue equal to the axial strain, while in the

unconfined compression configuration the specimen is free to expand radially (friction effects between specimen and compression platens are negligible). In the unconfined compression configuration the volumetric strains (and thus interstitial fluid outflow) are therefore controlled by the balance between the bulk and shear stiffness of the specimen.

Although the unconfined compression test subjects the specimens to 2-fold levels of axial strain, and a 10-fold ramp strain rate, as compared to the confined compression tests, the recorded peak stresses and equilibrium stresses are comparable for the two testing modes.

4.3. Variability in mechanical measurements

In agreement with the findings of Conrad et al. [28], we noted some degree of variability in stroma properties for samples excised from the same cervix but at different anatomical sites. On average, the maximum variability for samples taken from the same cervix was ±0.2 kPa for equilibrium and ±2.4 kPa for peak stress at 30% axial strain in unconfined compression. In general, there is a larger variability in tissue properties between patients (even patients with the same obstetric history) than between specimens from the same cervix. The standard variation in the stress levels reported in Table 3, Table 4 and Table 5 is due to the combined effects of variability among different patients and different cervical anatomical sites.

Preliminary histological studies were performed on stained stroma samples from human cervices obtained from hysterectomy specimens [37]. We were not able to identify a substantial degree of anisotropy in the arrangement of the collagen bundles; therefore, effects of specimen orientation were not expected to be significant, and during unconfined compression experiments no particular care was taken to align the transverse direction consistently among specimens. In other words, it was unknown if the lateral stretch measured from the video extensometer was associated with the circumferential, radial or any intermediate direction within the cervix. A large variability was noted in the lateral stretch measurements. If the tissue is anisotropic, then the lateral stretch will be dependent on tissue orientation and the variability in the findings can be easily explained. Possible effects of anisotropy on the tissue response are currently under investigation. For future experiments, we propose to cut the tissue into rectangular blocks and mark the orientation of the orthogonal anatomical planes. We believe that, by marking the cervix orientation on the testing specimens, variability will be reduced for the lateral stretch measurements.

4.4. Comparison between biochemistry analysis results and literature data

The biochemical measurements reported herein are in good agreement with previously reported biochemical results for human cervical tissue. Previous studies by Danforth et al. [23], Petersen et al. [15] and Rechberger et al. [14] reported significant differences in hydration and collagen extractability between nonpregnant and pregnant tissue samples. Table 7 summarizes these previous findings. All three investigations report that pregnant tissue is more hydrated than nonpregnant tissue. Furthermore, Petersen et al. concluded that collagen extractability is higher in NPPD tissue as compared to NPND tissue [15]. Rechberger et al. measured higher collagen extractability in pregnant tissue as compared to nonpregnant tissue [14]. Total collagen content and sulfated GAG measurements also fall within the range of data in the literature. Shimuzu et al. [44] measured 0.75% and 0.97% sulfated GAGs per dry weight of tissue for nonpregnant and

pregnant tissue, respectively. Petersen et al. [15] measured 94.4% and 73.6% collagen content per dry weight of tissue for NPND and NPPD cervical tissue, respectively.

Table 7. Summary of hydration and collagen extractability data available in the literature

Study	**Hydration non-pregnant**	**Hydration pregnant**	**Extractability NPND**	**Extractability NPPD**	**Extractability pregnant**
Danforth [23]	74.4%	78.4%	N/A	N/A	N/A
Petersen [15]	76.7%	79.5%	42.6%	49.5%	N/A
Rechberger [14]	81.1%	83.7%	Average: 68.8%		90.8%

5. Conclusions and future work

The mechanical properties of biological tissue can be drastically altered by relatively small modifications in its biochemistry. Nature modulates the mechanical properties of cervical tissue by subtle readjustments of its composition. The compliance of cervical stroma changes by orders of magnitude when the pregnancy nears term. A remarkable change in macroscopic properties is accomplished through subtle shifts in biochemical constituents. The total collagen content remains almost unchanged, while more significant changes are seen in collagen crosslinking and the relative quantities of sulfated GAGs and hyaluronic acid. The experimental results presented in Section 3 indicate that there is a correlation between obstetric history and biochemical and mechanical properties of the tissue. The results of this study also confirm that higher collagen extractability and hydration levels are associated with more compliant tissue behavior.

Future work will focus on improving the statistical power of this study, investigating the anisotropy of the tissue, exploring the electrical properties of individual classes of GAGs, improving the configuration of the tension specimens, and investigating the tissue's swelling properties. As stated in Section 4.3, we plan to investigate tissue anisotropy by loading marked tissue samples in different directions and measuring the lateral strain in both transverse directions. Studies by Petersen found that the mechanical properties were dependent on the direction of loading, where tissue cut in the longitudinal direction had a higher creep rate when compared to tissue cut in the circumferential direction [7]. We are also developing protocols to quantify the concentrations of distinct GAGs by fluorophore-assisted carbohydrate electrophoresis (FACE) [45]. Studies by Osmer et al. [16] and von Maillot et al. [9] investigated the importance of the relative concentrations of different GAGs during pregnancy and labor. It has been shown that the shift in GAG concentration among hyaluronic acid, dermatan sulfate and the chondroitin sulfates facilitates cervical softening during labor. It has also been shown that the finer structure of the GAG relating to the length of the GAG disaccharide chain and the degree of sulfation is important in the biomechanics of hydrated tissue (e.g. in cornea tissue [46] and osteoarthritic cartilage [47]). Our current DMB assay only measures total sulfated GAG content. The DMB assay does not characterize the electrostatic properties of the distinct GAG chains and cannot measure the hyaluronic acid content. The new FACE assay will allow us to overcome these limitations and will provide another means to differentiate the biomechanical properties of cervical specimens. Further, we will investigate the swelling properties of cervical stroma samples by exposing samples to different ionic bath concentrations and measuring their hydration. Currently, no studies in the literature have explored the electrical properties of

cervical stroma. Therefore, the FACE analysis and swelling studies will explore the role of the GAG electrical interactions in the mechanical integrity of the cervical stroma.

This study represents a first important step towards the attainment of an improved understanding of the complex interplay between the molecular structure of the tissue and its macroscopic mechanical properties. This study established mechanical testing and biochemical analysis protocols that will provide the foundation for our investigation of structure–property relations in cervical tissue.

Acknowledgements

We acknowledge the support of the Whitaker Foundation Biomedical Engineering Research Grant RG-02-0803, the National Science Foundation Graduate Research Fellowship, and the Society for Maternal Fetal Medicine – American Association of Obstetrician Gynecologists Foundation Scholarship. The authors thank Dr. Robert Kokenyesi and Dr. Phyllis Leppert for their kind help and guidance on the biochemistry analysis, Professor Alan Grodzinsky and Dr. Han-Hwa Hung for advice and guidance on the testing protocols. We also appreciate the support of the Departments of Gynecology and Pathology at the Tufts – New England Medical Center for providing hysterectomy specimens.

References

[1] J. Owen, J.D. Iams, J.C. Hauth. Vaginal sonography and cervical incompetence. Am J Obstet Gynecol, 188 (2) (2003), pp. 586–596

[2] G.J. Hofmeyr. Obstructed labor: using better technologies to reduce mortality. Int J Gynaecol Obstet, 85 (Suppl. 1) (2004), pp. S62–S72.

[3] M. Winkler, W. Rath. Changes in the cervical extracellular matrix during pregnancy and parturition. J Perinat Med, 27 (1999), pp. 45–61.

[4] P.C. Leppert. Anatomy and physiology of cervical ripening. Clin Obstet Gynecol, 38 (2) (1995), pp. 267–279.

[5] N. Uldbjerg, G. Ekman, A. Malmstrom, K. Olsson, U. Ulmsten. Ripening of the human uterine cervix related to changes in collagen, glycosaminoglycans, and collagenolytic activity. Am J Obstet Gynecol, 147 (6) (1983), pp. 662–666.

[6] D.N. Danforth. The fibrous nature of the human cervix, and its relation to the isthmic segment in gravid and nongravid uteri. Am J Obstet Gynecol, 53 (4) (1947), pp. 541–560.

[7] L.K. Petersen, H. Oxlund, N. Uldbjerg, A. Forman. In vitro analysis of muscular contractile ability and passive biomechanical properties of uterine cervical samples from nonpregnant women. Obstet Gynecol, 77 (5) (1991), pp. 772–776.

[8] H.P. Kleissl, M. Van Der Rest, F. Naftolin, F.H. Glorieux, A. De Leon. Collagen changes in the human uterine cervix at parturition. Am J Obstet Gynecol, 130 (1978), pp. 748–753.

[9] K. von Maillot, H.W. Stuhlsatz, H.H. Gentsch. Connective tissue changes in the human cervix in pregnancy and labour. D.A. Ellwood, A.B.M. Anderson (Eds.), The cervix in pregnancy and labour: clinical and biochemical investigations, Churchill Livingston Inc., New York (1981).

[10] P. Leppert, S. Yu. Elastin and collagen in the human uterus and cervix: biochemical and histological correlation. P.C. Leppert, J.F. Woessner (Eds.), The extracellular matrix of the uterus, cervix and fetal membranes: synthesis, degradation and hormonal regulation, Perinatology Press (1991).

[11] D.N. Danforth. The morphology of the human cervix. Clin Obstet Gynecol, 26 (1) (1983), pp. 7–13.

[12] P.W. Theobald, W. Rath, H. Kühnle, W. Kuhn. Histological and electron-microscopic examinations of collageneous connective tissue of the non-pregnant cervix, the pregnant cervix, and the pregnant prostaglandin-treated cervix. Arch Gynecol, 231 (1982), pp. 241–245.

[13] N. Uldbjerg, G. Ekman, A. Malmström, B. Sporrong, U. Ulmsten, L. Wingerup. Biochemical and morphological changes of human cervix after local application of prostaglandin E2 in pregnancy. The Lancet, 31 (1981), pp. 267–268.

[14] T. Rechenberger, N. Uldbjerg, H. Oxlund. Connective tissue changes in the cervix during normal pregnancy and pregnancy complicated by cervical incompetence. Obstet Gynecol, 71 (1988), pp. 563–567.

[15] L.K. Petersen, N. Uldbjerg. Cervical collagen in non-pregnant women with previous cervical incompetence. Eur J Obstet Gynecol Reprod Biol, 67 (1996), pp. 41–45.

[16] R. Osmers, W. Rath, M.A. Pflanz, W. Kuhn, H.W. Stuhlsatz, M. Szeverényi. Glycosaminoglycans in cervical connective tissue during pregnancy and parturition. Obstet Gynecol, 81 (1993), pp. 88–92.

[17] W. Rath, R. Osmers, M. Szeverényi, H.W. Stuhlsatz, W. Kuhn. Changes of glycosaminoglycans in cervical connective tissue. P.C. Leppert, J.F. Woessner (Eds.), The extracellular matrix of the uterus, cervix and fetal membranes: synthesis, degradation and hormonal regulation, Perinatology Press (1991).

[18] K.G. Danielson, H. Baribault, D.F. Holmes, H. Graham, K.E. Kadler, V. Iozzo. Targeted disruption of decorin leads to abnormal collagen fibril morphology and skin fragility. J Cell Biol, 136 (3) (1997), pp. 729–743.

[19] R. Kokenyesi, L.C. Armstrong, A. Agah, R. Artal, P. Bornstein. Thrombospondin 2 deficiency in pregnant mice results in premature softening of the uterine cervix. Biol Reprod, 70 (2004), pp. 385–390.

[20] M. Takemura, H. Itoh, N. Sagawa, S. Yura, D. Korita, K. Kakui et al. Cyclic mechanical stretch augments hyaluronan production in cultured human uterine cervical fibroblasts cells. Mol Hum Reprod, 11 (9) (2005), pp. 659–665.

[21] M. Yoshida, N. Sagawa, H. Itoh, S. Yura, M. Takemura, Y. Wada et al. Prostaglandin F2a, cytokines and cyclic mechanical stretch augment matrix metalloproteinase-1 secretion from cultured human uterine cervical fibroblast cells. Mol Hum Reprod, 8 (7) (2002), pp. 681–687.

[22] E.A. Friedman, B.H. Kroll. Computer analysis of labor progression III. Pattern variations by parity. J Reprod Med, 6 (4) (1971), pp. 63–67.

[23] D.N. Danforth, A. Veis, M. Breen, H.G. Weinstein, J.C. Buckingham, P. Manalo. The effect of pregnancy and labor on the human cervix: changes in collagen, glycoproteins, and glycosaminoglycans. Am J Obstet Gynecol, 120 (3) (1974), pp. 641–651.

[24] L. Granstrom, G. Ekman, A. Malmstrom. Insufficient remodeling of the uterine connective tissue in women with protracted labour. Br J Obstet Gynaecol, 116 (1994), pp. 502–513.

[25] R.E. Garfield, H. Maul, W. Maner, C. Fittkow, G. Olson, L. Shi et al. Uterine electromyography and light-induced fluorescence in the management of term and preterm labor. J Soc Gynecol Investig, 9 (2002), pp. 265–275.

[26] M.L.R. Harkness, R.D. Harkness. Changes in the physical properties of the uterine cervix of the rat during pregnancy. J Physiol, 148 (1959), pp. 524–547.

[27] S.J. Stys, W.H. Clewell, G. Meschia. Changes in cervical compliance at parturition independent of uterine activity. Am J Obstet Gynecol, 130 (4) (1978), pp. 414–418.

[28] J.T. Conrad, R.D. Tokarz, J.F. Williford. Anatomic site and stretch modulus in the human cervix. F. Naftolin, P.G. Stubblefield (Eds.), Dilatation of the uterine cervix: connective tissue biology and clinical management, Raven Press, New York (1980), pp. 255–264.

[29] E.H. Bishop. Pelvic scoring for elective induction. Obstet Gynecol, 24 (2) (1964), pp. 266–268.

[30] T. Bakke. Cervical consistency in women of fertile age measured with a new mechanical instrument. Acta Obstet Gynec Scand, 53 (1974), pp. 293–302.

[31] D. Cabrol. Cervical distensibility changes in pregnancy, term, and preterm labor. Semin Perinatol, 15 (2) (1991), pp. 133–139.

[32] E. Mazza, A. Nava, M. Bauer, R. Winter, M. Bajka, G.A. Holzapfel. Mechanical properties of the human uterine cervix: An in vivo study. Med Image Anal, 10 (2) (2006), pp. 125–136.

[33] G.N. Kiefer, K. Sundby, D. McAllister, N.G. Shrive, C.B. Frank, T. Lam et al. The effect of cryopreservation on the biomechanical behavior of bovine articular cartilage. J Orthop Res, 7 (4) (1989), pp. 494–501.

[34] E.M. Parsons, M.C. Boyce, D.M. Parks, M. Weinberg. Three-dimensional large-strain tensile deformation of neat and calcium carbonate-filled high-density polyethylene. Polymer, 46 (2005), pp. 2257–2265.

[35] J.F. Woessner. Determination of hydroxyproline in connective tissues. D.A. Hall (Ed.), Methodology of connective tissue research, Joynson–Bruvvers Ltd., Oxford (1976), p. 976.

[36] R.W. Farndale, C.A. Sayers, A.J. Barett. A direct spectrophotometric microassay for sulfated glycosaminoglycans in cartilage cultures. Connect Tissue Res, 9 (1982), pp. 247–248.

[37] Febvay S. A three-dimensional constitutive model for the mechanical behavior of cervical tissue. Master's thesis, Massachusetts Institute of Technology, Cambridge, MA; 2003.

[38] S.R. Eisenberg, A.J. Grodzinsky. Swelling of articular cartilage and other connective tissue: electromechanochemical forces. J Orthop Res, 3 (2) (1985), pp. 148–159.

[39] P.M. Bursac, T.W. Obitz, S.R. Eisenberg, D. Stamenovic. Confined and unconfined stress relaxation of cartilage: appropriateness of a transversely isotropic analysis. J Biomech, 32 (1999), pp. 1125–1130.

[40] A.C. Chen, W.C. Bae, R.M. Schinagl, R.L. Sah. Depth- and strain-dependent mechanical and electromechanical properties of full-thickness bovine articular cartilage in confined compression. J Biomech, 34 (2001), pp. 1–12.

[41] G.A. Ateshian, W.H. Warden, J.J. Kim, R.P. Grelsamer, V.C. Mow. Finite deformation biphasic material properties of bovine articular cartilage from confined compression experiments. J Biomech, 30 (1997), pp. 1157–1164.

[42] R.M. Aspden. Collagen organisation in the cervix and its relation to mechanical function. Collagen Rel Res, 8 (1988), pp. 103–112.

[43] M. House, A. Paskaleva, K. Myers, S. Febvay, S. Socrate. The biomechanics of cervical funneling: the effect of stroma properties, anatomic geometry and pelvic forces on funnel formation. Am J Obstet Gynecol, 191 (6) (2004), p. S17.

[44] T. Shimizu, M. Endo, Z. Yosizawa. Glycoconjugates (glycosaminoglycans and glycoproteins) and glycogen in the human cervix uteri. Tohoku J Exp Med, 131 (1980), pp. 289–299.

[45] A. Calabro, V.C. Hascall, R.J. Midura. Adaptation of FACE methodology for microanalysis of total hyaluronan and chondroitin sulfate composition from cartilage. Glycobiology, 10 (3) (2000), pp. 283–293.

[46] A.H. Plaas, L.A. West, E.J.A. Thonar, A.Z. Karcioglu, C.J. Smith, G.K. Klintworth et al. Altered fine structures of corneal and skeletal keratin sulfate and chondroitin/dermatan sulfate in macular corneal dystrophy. J Biol Chem, 276 (43) (2001), pp. 39788–39796.

[47] A.H. Plaas, L.A. West, S. Wong-Palms, F.R. Nelson. Glycosaminoglycan sulfation in human osteoarthritis. J Biol Chem, 273 (20) (1998), pp. 12642–12649.